



Frontiers article

A vacuum ultraviolet photoionization study on the isomerization, decomposition, and molecular mass growth processes in solid nitromethane (CH₃NO₂)

Santosh K. Singh, Ralf I. Kaiser*

W.M. Keck Research Laboratory in Astrochemistry, University of Hawaii at Manoa, Honolulu, HI 96822, USA
 Department of Chemistry, University of Hawaii at Manoa, Honolulu, HI 96822, USA



ARTICLE INFO

Keywords:

Nitromethane
 Isomerization
 Mass spectrometry
 Photoionization

ABSTRACT

In this Feature Article, we highlight the crucial findings from experimental and theoretical studies investigating the dissociation mechanisms of condensed phase nitromethane (CH₃NO₂), a model compound of nitrohydrocarbon (R-NO₂) based energetic material. Our findings on intriguing isomerization, decomposition and molecular mass growth pathways of nitromethane are placed into perspective by exploiting complementary spectroscopy probes such as Fourier Transform Infrared Spectroscopy (FTIR), Electron Paramagnetic Resonance (EPR), and single-photon isomer selective photoionization reflectron time-of-flight mass spectrometry (PI-ReTOF-MS) in conjunction with quantum chemical calculations. These investigations unravel the isomerization of nitromethane to exotic isomers such as aci-nitromethane, nitrosomethanol, and N-hydroxyoxaziridine. Evidence of non-equilibrium decomposition channels involving suprathreshold oxygen, hydrogen and carbene formation are also revealed. Finally, involvement of these radical species in molecular mass growth processes leading to higher molecular weight products are emphasized. Benchmark studies established from a 'simple' nitromethane system are highly beneficial to predict the decomposition mechanisms of 'real' explosives.

1. Introduction

For the last decades, the fundamental isomerization, (unimolecular) decomposition, and molecular mass growth processes of nitromethane (CH₃NO₂; **1**) have received extensive interest from the physical chemistry [1,2], theoretical chemistry [3–5], and material science community [6,7] since nitromethane represents a model compound of nitrohydrocarbon-based (R-NO₂) energetic material covering explosives [8–11], propellants [12,13], and high-performance fuel additives for detonation systems and internal combustion engines (Fig. 1) [14]. A detailed knowledge of the (unimolecular) decomposition pathways of nitromethane and of the consecutive reactions of the radicals formed in these processes are critical to predict the performance [15,16], aging behaviour [17,18], and sensitivity to heat and shock of energetic materials [1,6,7,19–21]. This comprehension is also valuable to simulate the time-dependence during the ignition stage of explosives, to dispose (aged) energetic materials securely under controlled conditions, and to design novel, shock-insensitive energetic materials [22,23]. However,

the unraveling of the decomposition pathways, isomerization processes, and molecular mass growth processes of nitromethane still signifies ample challenges for experimentalists, theoreticians, and modelers contemplating the non-equilibrium conditions under which these reactions often transpire [24–30]. This requires first an understanding of the underlying mechanisms at the most fundamental, microscopic level exploiting single nitromethane molecules in the gas phase, but also in the condensed phase so that the initially formed molecular and radical fragments such as carbon-, oxygen-, and nitrogen-centered radicals may react with the neighboring molecules.

The unimolecular decomposition of nitromethane has been comprehensively explored in the gas phase exploiting ultraviolet photodissociation (UVPD) and infrared multi photon dissociation (IRMPD) [31–45]. Utilizing supersonic molecular beams, these studies revealed two key channels: (1) a unimolecular decomposition of nitromethane (CH₃NO₂; **1**) to the methyl radical (CH₃) and to nitrogen dioxide (NO₂) [reaction (1)] and (2) a roaming-mediated nitromethane (CH₃NO₂; **1**) – methyl nitrite (CH₃ONO; **2**) isomerization along with a

* Corresponding author at: W.M. Keck Research Laboratory in Astrochemistry, University of Hawaii at Manoa, Honolulu, HI 96822, USA and Department of Chemistry, University of Hawaii at Manoa, Honolulu, HI 96822, USA.

E-mail address: ralfk@hawaii.edu (R.I. Kaiser).

<https://doi.org/10.1016/j.cplett.2021.138343>

Received 2 October 2020; Received in revised form 6 January 2021; Accepted 8 January 2021

Available online 11 January 2021

0009-2614/© 2021 Elsevier B.V. All rights reserved.

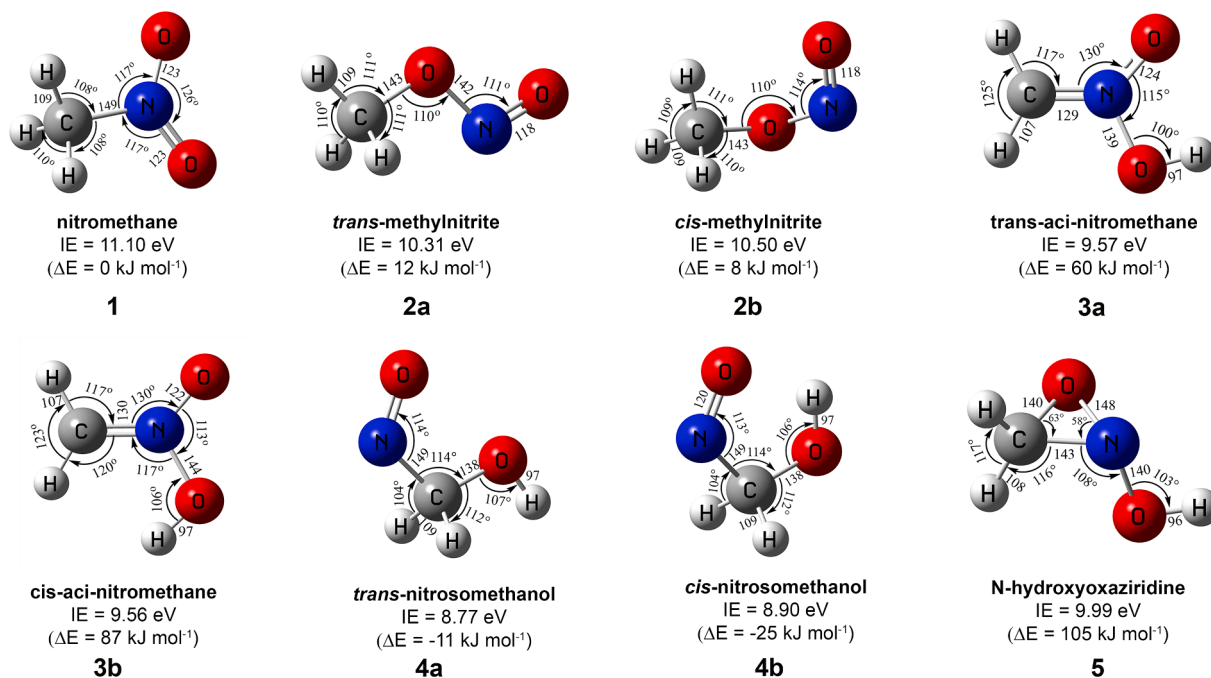


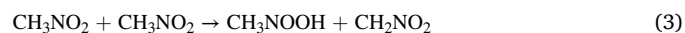
Fig. 1. Key structural isomers of nitromethane (CH_3NO_2 ; **1**) along with their relative energies (in kJ mol⁻¹) and adiabatic ionization energies (in eV): methylnitrite (CH_3ONO ; **2**), aci-nitromethane ($\text{H}_2\text{C}=\text{N}(\text{O})\text{OH}$; **3**), nitrosomethanol ($\text{H}_2\text{C}(\text{NO})\text{OH}$; **4**) and N-hydroxyoxaziridine ($c\text{-CH}_2\text{NOH}(\text{O})$; **5**) adapted from reference [82].

unimolecular decomposition through a radical mechanism forming a methoxy radical (CH_3O) and nitrogen monoxide (NO) [reaction (2a)] and via a molecular elimination pathway resulting in formaldehyde (H_2CO) plus nitrosyl hydride (HNO) [reaction (2b)]. [46] Note that upon photoexcitation of the $\pi \rightarrow \pi^*$ transition, nitrogen dioxide (NO_2) was found to be formed in its electronic ground (X^2A_1) and first excited state (A^2B_2) [32]. Recently, a three-body dissociation pathway to the methyl radical, nitrogen monoxide, and atomic oxygen was proposed as well. State-selective ion imaging studies of the nitrogen monoxide fragment by Suits et al. support roaming mediated reaction dynamics [36]; Lin et al. proposed that the $1 \rightarrow 2$ isomerization (reaction (2)) via a roaming transition state dominates at pressures below 2 Torr, whereas the radical decomposition pathway (reaction (1)) becomes more important at higher pressures [47]. At higher ultraviolet photon fluxes, decomposition of the rovibrationally excited methyl radicals and/or their subsequent photolysis lead to fragmentation forming highly reactive carbene (CH_2) and methylidyne (CH) radicals [48]. Although predicted theoretically [4], high energy pathways do not compete under IRMPD and UVPD conditions. These include a hydrogen atom migration from the methyl group of nitromethane (CH_3NO_2 ; **1**) to an oxygen atom via a barrier of 314 kJ mol⁻¹ forming aci-nitromethane ($\text{H}_2\text{C}=\text{N}(\text{O})\text{OH}$; **3**), an oxygen atom shift in aci-nitromethane ($\text{H}_2\text{C}=\text{N}(\text{O})\text{OH}$; **3**) to nitrosomethanol ($\text{H}_2\text{C}(\text{NO})\text{OH}$; **4**), and/or ring closure of aci-nitromethane ($\text{H}_2\text{C}=\text{N}(\text{O})\text{OH}$; **3**) to N-hydroxyoxaziridine ($c\text{-CH}_2\text{NOH}(\text{O})$; **5**).



In the solid state, only a few experimental and computational studies were carried out. Rebbert and Slagg [49] and Bielski et al. [50] performed a mercury arc photolysis of liquid nitromethane and nitromethane ice at 77 K. These studies exposed a carbon–nitrogen single bond cleavage in **1** as the initial step accompanied by the detection of methyl radicals and nitrogen dioxide (reaction (1)). A broad-band photolysis of nitromethane covering 240 to 360 nm in a low temperature argon matrix revealed the $1 \rightarrow 2$ isomerization as the primary

pathway [51,52]. Extended photon exposure resulted in higher order products such as a formaldehyde (H_2CO) – nitrosyl hydride (HNO) bonded complex as expected in the molecular pathway via reaction (2b) and also in the formation of nitrosomethanol ($\text{H}_2\text{C}(\text{NO})\text{OH}$; **4**) [51]. Water (H_2O) - isocyanic acid (HCNO) complexes were detected at prolonged radiation exposure. Jacox et al. proposed that the detected carbon monoxide (CO) at extended stages of the irradiation could be explained by the photodecomposition of formaldehyde formed via reaction (2b) [52]. The thermal decomposition of condensed phase nitromethane was also explored theoretically via molecular dynamics calculations [5,53]. At temperatures of 2,000 to 2,500 K, the $1 \rightarrow 2$ isomerization dominated; an intermolecular hydrogen transfer in a nitromethane dimer ($(\text{CH}_3\text{NO}_2)_2$) lead to the N-hydroxy-nitrosomethane radical (CH_3NOOH) plus a nitromethyl radical (CH_2NO_2) at temperatures reaching 3,000 K (reaction (3)). Further, an intermolecular hydrogen shift in nitromethane yielded aci-nitromethane ($\text{H}_2\text{C}=\text{N}(\text{O})\text{OH}$; **3**), which decomposes to water (H_2O) and isocyanic acid (HCNO) (reaction (4)). The dynamics simulations proposed an alternative pathway to water formation via an initial hydroxyl radical (OH) formation from N-hydroxy-nitrosomethane (CH_3NOOH) followed by recombination with atomic hydrogen. Most important, these simulations predicted that besides these smaller molecules, the decomposition result in (hitherto unidentified) complex organic molecules containing up to 70% of the carbon and nitrogen atoms of nitromethane. Considering that the simulations involved timescales of only up to 200 ps [5], only products carrying up to three carbon atoms were formed involving molecular mass growth processes through hydrogen atom transfer reactions and short-lived radicals along with organics carrying the C-N-C-N chain moiety.



However, no comprehensive reaction mechanisms have been developed portraying the decomposition of nitromethane (CH_3NO_2 ; **1**) together with the reactions of the carbon, nitrogen, and oxygen-bearing radical species formed in these processes. Whereas molecular beam studies provided exceptional information on the dynamics of the

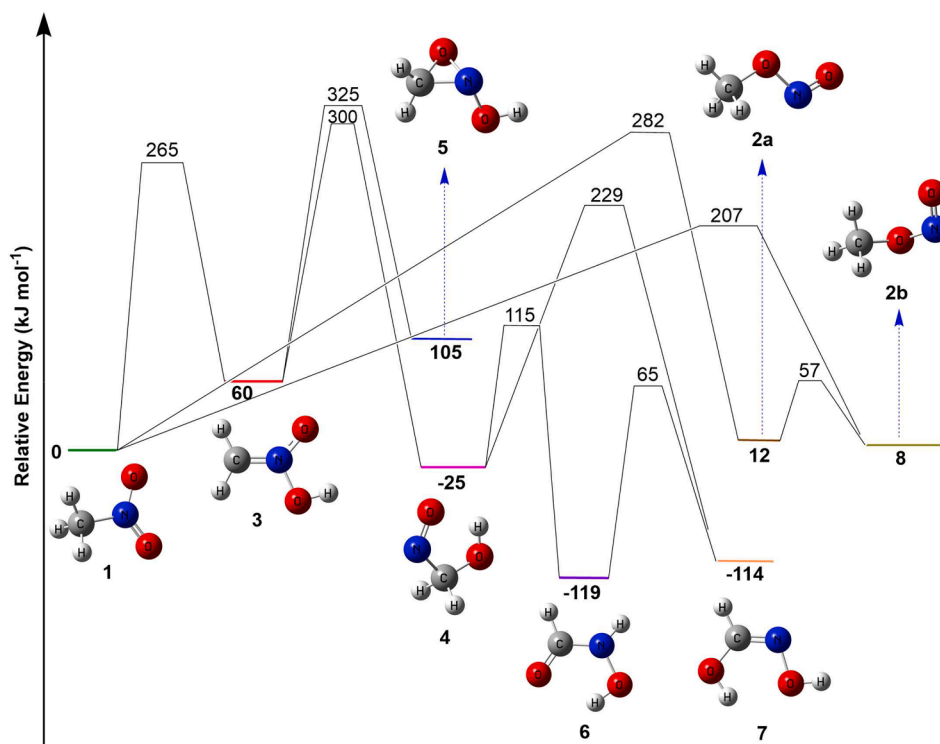


Fig. 2. Isomerization of distinct isomers of nitromethane (CH_3NO_2 ; 1) calculated at the B3LYP/cc-pVTZ//CCSD(T)/CBS level of theory. Adapted from references [79,80].

decomposition of 1 under single collision conditions (reactions (1) and (2)), the decomposition of energetic materials in the solid state is expected to be more complex as evident from theoretically predicted intermolecular hydrogen atom transfer reactions, ‘dimerization’ reactions, and the formation of higher-molecular weight molecules of yet unknown structure. Further, these processes might involve more exotic isomers beyond nitromethane (CH_3NO_2 ; 1) and methylnitrite (CH_3ONO ; 2): aci-nitromethane ($\text{H}_2\text{C}=\text{N}(\text{O})\text{OH}$; 3), nitrosomethanol ($\text{H}_2\text{C}(\text{NO})\text{OH}$; 4), and N-hydroxyoxaziridine ($c\text{-CH}_2\text{NOH}(\text{O})$; 5) (Fig. 1). Hence, new experimental investigations of the decomposition of nitromethane in the condensed phase and the subsequent reaction pathways of the carbon, nitrogen, and oxygen-bearing radicals are desired.

In this *Feature Article*, recent accomplishments on the isomerization of nitromethane (CH_3NO_2 ; 1) to distinct isomers beyond methylnitrite (CH_3ONO ; 2) - aci-nitromethane ($\text{H}_2\text{C}=\text{N}(\text{O})\text{OH}$; 3), nitrosomethanol ($\text{H}_2\text{C}(\text{NO})\text{OH}$; 4), and N-hydroxyoxaziridine ($c\text{-CH}_2\text{NOH}(\text{O})$; 5) - are presented (2.1.). Latest achievements on classical and non-equilibrium decomposition pathways of nitromethane (CH_3NO_2 ; 1) involving suprathreshold hydrogen atoms (H), oxygen (O), and carbene (CH_2) pursue this section (2.2. and 2.3.). Finally, the role of these species in molecular mass growth processes are highlighted and compared to recent molecular dynamics simulations (2.4.). This is achieved by exposing thin films of nitromethane (CH_3NO_2 ; 1) and mixtures with D3-nitromethane (CD_3NO_2 ; 1) to ionizing radiation in form of energetic electrons and Lyman α (10.20 eV) photons at 5 K under ultra high vacuum (UHV; 10^{-11} Torr) conditions. Considering the low temperature of 5 K, the ice target having a thickness in the range of 380–450 nm, represents a ‘closed system’ as reaction products - including atomic and molecular hydrogen - remain trapped in the cryogenic sample. Previous investigations suggested that the molecular packing of the solid nitromethane (CH_3NO_2 ; 1) does not change with the temperature from 4.2 K to the melting point [54], making the current experimental work relevant to higher temperature as well. During the exposure to ionizing radiation, the chemical modifications of the target is monitored via Fourier Transform Infrared (FTIR) spectroscopy on line and in situ; this

technique assists in the identification of newly formed *small molecules* and *functional groups* of complex organics [55]. These studies assist extracting concepts on the reaction mechanisms, products, and intermediates in the decomposition of nitromethane and of the radical reactions involved in the condensed phase. After the exposure to ionizing irradiation, the samples are warmed up (temperature programmed desorption; TPD), and the subliming molecules are detected in the gas phase via vacuum ultraviolet (VUV) single photon ionization (PI) of the subliming neutral molecules coupled with a reflectron time-of-flight mass spectrometer (PI-ReTOF-MS) [56–65] with tunable VUV light generated by resonance enhanced sum ($2\omega_1+\omega_2$) and difference ($2\omega_1-\omega_2$) frequency nonlinear mixing [66,67]. Compared to electron impact ionization, PI-ReTOF-MS represents a versatile approach to selectively detect and to photoionize distinct isomers ideally fragment-free based on their ionization energies thus gaining a comprehensive inventory of the *isomer selective* decomposition and reaction products. These data provided compelling evidence of multiple non-equilibrium reaction mechanisms, products, and intermediates, which were found to be quite distinct from those observed in the decomposition of nitromethane in the gas phase under collision less conditions. Hence, these data eventually aid the fundamental understanding of the (non-equilibrium) decomposition of energetic materials, inherent energy transfer processes, and mass growth mechanisms involving the generation of carbon-, nitrogen-, and oxygen-centered radicals.

2. Reaction mechanisms

2.1. Structural isomers & isomerization pathways

Historically, the aci-nitromethane isomer ($\text{H}_2\text{C}=\text{N}(\text{O})\text{OH}$; 3) was proposed to exist in the gas phase and detected tentatively via neutralization - reionization mass spectrometry by Egsgaard et al. in 1989 [68]. In the condensed phase, it was inferred as the initial reaction product in the protonation of the nitromethyl anion (H_2CNO_2^-) [69]. More recently, calculations of Dhanya et al. [70] suggested that the hydroxyl radical

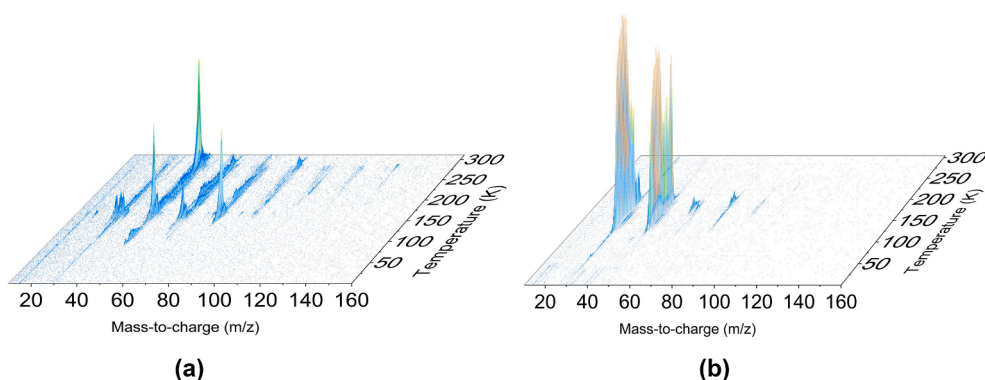


Fig. 3. (a) PI-ReTOF-MS data of the newly formed products subliming into the gas phase from irradiated nitromethane (CH_3NO_2 ; **1**) ice as a function of temperature at a photon energy of 10.49 eV. (b) PI-ReTOF-MS data of the newly formed products subliming into the gas phase from irradiated methane – nitrogen dioxide ice as a function of temperature at a photon energy of 10.49 eV.

fragment (OH) in photolysis experiments originated from the acinitromethane isomer (**3**). Sung et al. [71] exploited a quantum mechanics/molecular mechanics approach to explore the reduction of nitrogen oxides with acetic acid and acetaldehyde in the Barium Y zeolite; this work identified (**3**) as one of the key intermediates. Further, Wang et al. [72] utilized the ONIOM (our own n-layered integrated molecular orbital and molecular mechanics) approach to investigate the chemistry of nitromethane (CH_3NO_2 ; **1**) and the isomerization to (**3**) confined inside armchair (5, 5) single-walled carbon nanotubes (CNT). Compared to a gas phase barrier of 260 kJ mol^{-1} , the barrier to isomerization was reduced to 239 kJ mol^{-1} by confinement effects; likewise the barrier to isomerization from nitromethane (CH_3NO_2 ; **1**) to methyl nitrite (CH_3ONO ; **2**) decreased from 272 to 193 kJ mol^{-1} .

The nitrosomethanol isomer ($\text{H}_2\text{C}(\text{NO})\text{OH}$; **4**) was first observed by Mueller and Huber [73]. Through excitation of the $S_1(n\pi^*)$ transition at 365 nm of matrix isolated methyl nitrite (CH_3ONO ; **2**), a hydrogen-bonded formaldehyde (H_2CO) - nitrosyl hydride (HNO) complex was formed. The photolysis of this complex produced either the *trans* ($\lambda = 345 \text{ nm}$) or the *cis* ($\lambda > 645 \text{ nm}$) isomer of (**4**). Yu and Liu [74] expanded

the aforementioned photochemical study computationally and predicted that the photolysis of the complex should produce *trans* (**4**), which can further isomerize to *cis* (**4**) at $\lambda > 645 \text{ nm}$. Kalkanis and Shields [75] predicted that (**4**) represented the dominant reaction product of the hydroxymethyl (CH_2OH) – nitrogen monoxide (NO) radical–radical recombination. The calculations were later expanded to the MP4SDTQ/6-311 + G(d,p) level with MP2(full)/6-31G(d,p) geometry optimization by Shin et al. [76]

The N-hydroxyoxaziridine ($c\text{-CH}_2\text{NOH}(\text{O})$; **5**) was initially predicted to exist based on theoretical studies by McKee et al. [4] Subsequent studies by Hu et al. [77] at the G2MP2//B3LYP/6-311++G(2d,2p) level of theory qualitatively agree with those by McKee and revealed that (**5**) can be formed from (**3**) via a 229 kJ mol^{-1} barrier. This isomer is 121 kJ mol^{-1} less stable than nitromethane (**1**), but it resides in a deep potential energy minimum with barriers to isomerization into (**3**) and (**4**) beyond 190 kJ mol^{-1} . Most recently, Zhang et al. [78] also predicted the existence of (**5**) computationally.

Recently, by exposing nitromethane (CH_3NO_2 ; **1**) ices to ionizing radiation at 5 K, fundamental isomerization processes of nitromethane

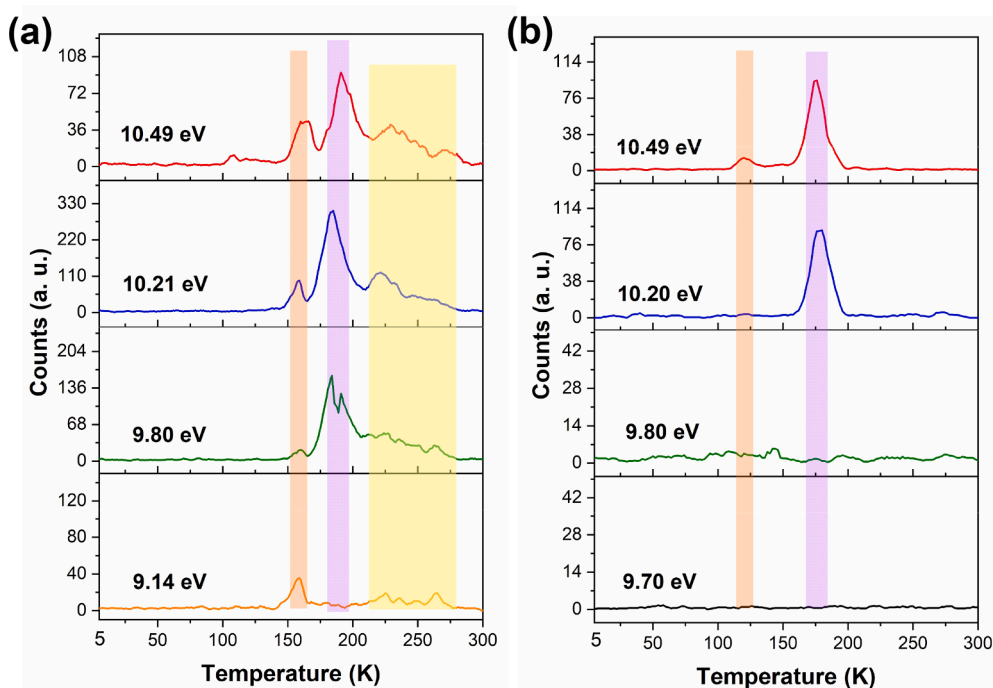


Fig. 4. (a) TPD profiles of irradiated nitromethane ice recorded at $m/z = 61$ at photon energies of 10.49, 10.21, 9.80 and 9.14 eV. (b) TPD profiles of irradiated methane – nitrogen dioxide ice recorded at $m/z = 61$ at photon energies of 10.49, 10.20, 9.80 and 9.70 eV. Adapted from references [79,82].

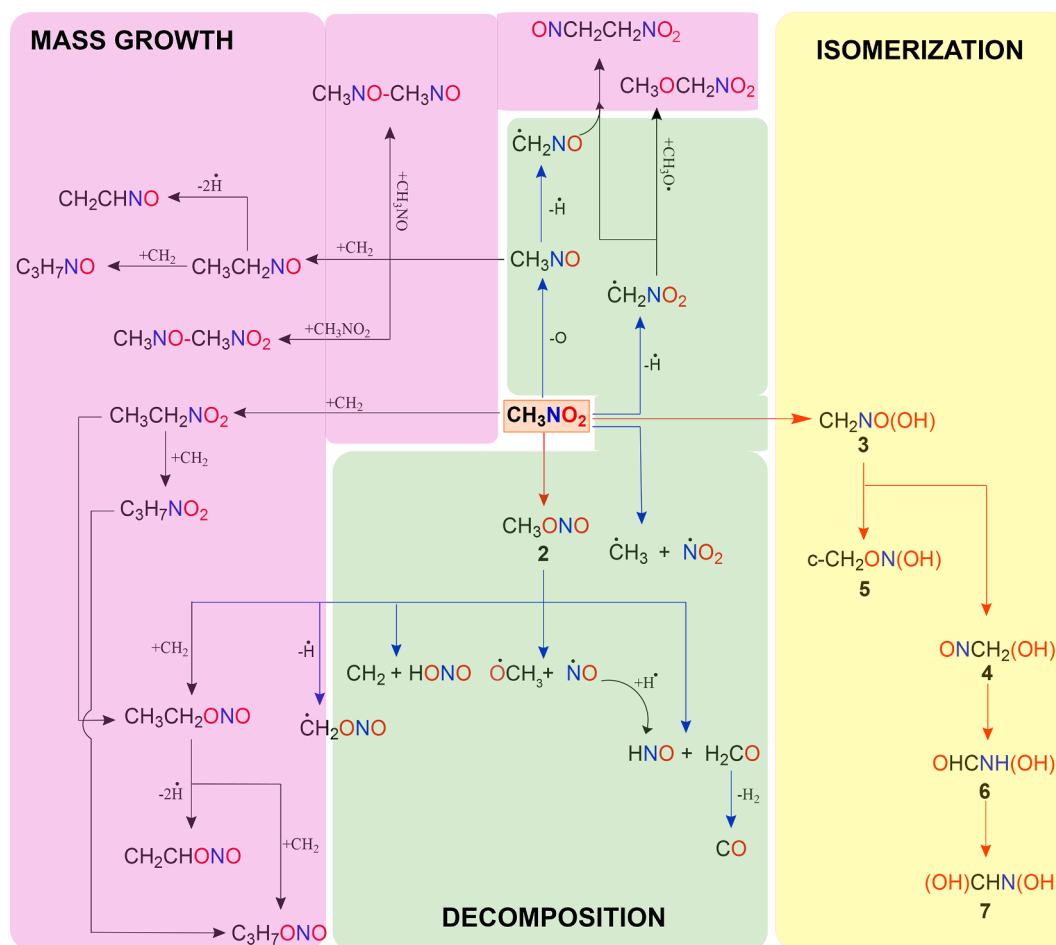


Fig. 5. Key isomerization (yellow), decomposition (green), and molecular mass growth pathways (pink) in nitromethane ices. (For interpretation of the references to colour in this figure legend, the reader is referred to the web version of this article.)

(CH_3NO_2 ; **1**) were exploited through a detection of the isomerization products by PI-ReTOF-MS of the subliming products employing tunable vacuum ultraviolet light [79]. Validated by electronic structure calculations, nitromethane (CH_3NO_2 ; **1**) was found to isomerize to methyl nitrite (CH_3ONO ; **2**) and also *via* hydrogen migration to the acinitromethane ($\text{H}_2\text{C}=\text{N}(\text{O})\text{OH}$; **3**) isomer. The later (isomer **3**) could undergo hydroxyl group (OH) migration to form nitrosomethanol ($\text{H}_2\text{C}(\text{NO})\text{OH}$; **4**) or ring closure to generate N-hydroxyoxaziridine ($c\text{-CH}_2\text{NOH}(\text{O})$; **5**). In detail, starting from nitromethane (CH_3NO_2 ; **1**), two initial isomerization pathways were identified (Figs. 1 and 2). The first pathway comprises the isomerization to *cis*- or *trans*-methyl nitrite (CH_3ONO ; **2a/b**) involving transition states located at 207 and 282 kJ mol^{-1} with respect to (**1**); **2a** and **2b** may interconvert through a barrier of 45 kJ mol^{-1} . The second isomerization pathway from (**1**) to acinitromethane ($\text{H}_2\text{C}=\text{N}(\text{O})\text{OH}$; **3**) passing a barrier of 265 kJ mol^{-1} ; this isomer was found to be 60 kJ mol^{-1} less stable than (**1**). Acinitromethane ($\text{H}_2\text{C}=\text{N}(\text{O})\text{OH}$; **3**) was predicted to undergo a ring closure by overcoming a 265 kJ mol^{-1} barrier to N-hydroxyoxaziridine ($c\text{-CH}_2\text{NOH}(\text{O})$; **5**). Alternatively, acinitromethane ($\text{H}_2\text{C}=\text{N}(\text{O})\text{OH}$; **3**) could isomerize *via* hydroxyl (OH) group migration from the nitrogen to the carbon atom *via* a lower barrier (240 kJ mol^{-1}) to rearrange to nitrosomethanol ($\text{H}_2\text{C}(\text{NO})\text{OH}$; **4**); this isomer is more stable by 25 kJ mol^{-1} with respect to nitromethane (CH_3NO_2 ; **1**).

Experimentally, thin nitromethane ices were subjected to ionizing radiation in form of energetic electrons [55,79,80] and Lyman α photons [81]. The exposed ices are then subjected to temperature programmed desorption (TPD) to sublime the newly formed molecules into the gas phase, where they are then photoionized. Ionized CH_3NO_2 species (m/z

= 61) were explored between photon energies from 10.49 eV to 9.14 eV (Figs. 3a and 4a). First, accounting for distinct ionization energies (Fig. 4a), the sublimation event around 250 K could be linked to *cis*/*trans* nitrosomethanol ($\text{H}_2\text{C}(\text{NO})\text{OH}$; **4**). Toward lower temperatures, the sublimation event at 185 K vanishes when switching from 9.80 eV to 9.14 eV. This sublimation region could be attributed to acinitromethane ($\text{H}_2\text{C}=\text{N}(\text{O})\text{OH}$; IE = 9.56 eV; **3**) and/or formohydroxamic acid (HCONHOH ; IE = 9.42–9.66 eV, **6–7**) isomers as their ionization energies exist between 9.80 and 9.14 eV. Based on the potential energy surface depicted in Fig. 2, it could be suggested that acinitromethane ($\text{H}_2\text{C}=\text{N}(\text{O})\text{OH}$; **3**) might originate from nitromethane (CH_3NO_2 ; **1**), while formohydroxamic acid (HCONHOH ; **6–7**) could form from nitrosomethanol ($\text{H}_2\text{C}(\text{NO})\text{OH}$; **4**) itself can only originate from acinitromethane ($\text{H}_2\text{C}=\text{N}(\text{O})\text{OH}$; **3**) via hydroxyl group migration therefore, we can link the sublimation profile peaking at 185 K to the acinitromethane ($\text{H}_2\text{C}=\text{N}(\text{O})\text{OH}$; **3**) isomer with possible contributions from formohydroxamic acid (HCONHOH). Combined with the infrared spectroscopic observation of methyl nitrite (CH_3ONO ; **2**), the exposure of solid nitromethane (CH_3NO_2 ; **1**) to energetic radiation is dictated by two isomerization processes: nitromethane (CH_3NO_2 ; **1**) \rightarrow methyl nitrite (CH_3ONO ; **2**) and nitromethane (CH_3NO_2 ; **1**) \rightarrow acinitromethane ($\text{H}_2\text{C}=\text{N}(\text{O})\text{OH}$; **3**) \rightarrow nitrosomethanol ($\text{H}_2\text{C}(\text{NO})\text{OH}$; **4**) thus involving critical hydrogen and hydroxyl group migrations and revealing the involvement of at least two exotic isomers in the decomposition of nitromethane: acinitromethane ($\text{H}_2\text{C}=\text{N}(\text{O})\text{OH}$; **3**) and nitrosomethanol ($\text{H}_2\text{C}(\text{NO})\text{OH}$; **4**). The importance of hydrogen shifts in the isomerization in the condensed phase was also verified via the

nitrosomethane (CH₃NO) – formaldehyde oxime isomer (H₂NCOH) pair [80].

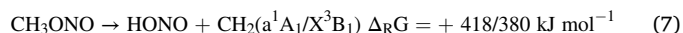
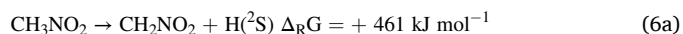
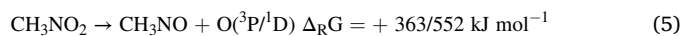
Finally, the chiral, thermodynamically least stable isomer - N-hydroxyoxaziridine (c-CH₂NOH(O); 5) – was only detected very recently. Recall that N-hydroxyoxaziridine (c-CH₂NOH(O); 5) is connected via a substantial barrier ranging of 265 kJ mol⁻¹ to the thermodynamically favored aci-nitromethane (H₂C=N(O)OH; 3). Formally, this isomerization involves a rotation of the CH₂ moiety perpendicularly to the –NOH fragment followed by a migration of the oxygen atom to form a carbon–oxygen σ bond and hence a three-membered ring through a [1,2] sigmatropic shift. However, the kinetic and thermodynamical stability of aci-nitromethane (H₂C=N(O)OH; 3) compared to N-hydroxyoxaziridine (c-CH₂NOH(O); 5) along with the preferred isomerization of aci-nitromethane (H₂C=N(O)OH; 3) to nitrosomethanol (H₂C(NO)OH; 4) through a hydroxyl group migration from the nitrogen atom to the carbon atom reveals the necessity of an alternative synthetic route to N-hydroxyoxaziridine (c-CH₂NOH(O); 5). This was achieved by exploiting PI-ReTOF-MS of subliming reaction products of radiolyzed methane (CH₄), D₄-methane (CD₄) or ¹³C-methane (¹³CH₄) plus nitrogen dioxide (NO₂) ices (Fig. 3b).[82] Bond-cleavage processes in (isotopically labeled) methane were initiated by exposing these ices to energetic electrons at doses of 1.2 ± 0.2 eV per molecule on average. N-hydroxyoxaziridine (c-CH₂NOH(O); 5) represents one of the simplest members of an oxaziridines [83–89] and was prepared eventually via addition of carbene (CH₂) to the nitrogen–oxygen double bond of nitrous acid (HONO) formed in situ via hydrogen atom recombination with nitrogen dioxide (NO₂) [82]. By systematically tuning the photoionization energies from 10.49 eV to 10.20 eV and 9.80 eV to 9.70 eV, N-hydroxyoxaziridine (c-CH₂NOH(O); 5) was eventually identified by selectively ionizing distinct CH₃NO₂ isomers (Fig. 4b).

2.2. Classical decomposition pathways

Having identified four structural isomers of nitromethane (CH₃NO₂; 1) [79,82], we are commenting now on ‘classical’ decomposition pathways ‘expected’ from aforementioned gas phase decomposition studies under molecular beam conditions (reactions (1) and (2)). By exposing thin films of nitromethane (CH₃NO₂; 1) to ionizing radiation at 5 K, the infrared data revealed first order kinetics and the initial isomerization of nitromethane (CH₃NO₂; 1) to methyl nitrite (CH₃ONO; 2). The infrared studies documented that methyl nitrite (CH₃ONO; 2) decomposed via two competing pathways involving the radical route and the molecular fragmentation mechanism into the methoxy radical (CH₃O) plus nitrogen monoxide (NO) (reaction (2a)) and into formaldehyde (H₂CO) plus nitrosyl hydride (HNO) (reaction (2b)), respectively (Fig. 5) [80,81]. The decomposition of nitromethane (CH₃NO₂; 1) into methyl radicals (CH₃) plus nitrogen dioxide (NO₂) (reaction (1)) was traced via electron spin resonance (ESR) spectroscopy (Fig. 5) [90]. It is important to highlight that the overall branching ratios of (1) vs. (2a) and (2b) strongly depend on the source of ionizing radiation (electrons versus photons) and also the photolysis wavelength [55,79,81,90]. Consequently, we can conclude that the molecular (1) and radical fragmentation pathways (2a/2b) are important both in the gas phase and condensed phase (ices) decomposition of nitromethane (CH₃NO₂; 1) albeit with different branching ratios. Considering that the gas phase experiments on the decomposition of nitromethane (CH₃NO₂; 1) were conducted under molecular beam conditions and the primary products fly apart undisturbed to the detector, i.e. they cannot react back, the solid matrix at 5 K may critically influence these branching ratios. This has been documented in experiments exposing methanol (CH₃OH) – nitrogen monoxide (NO) ices at 5 K to ionizing radiation [91]. Considering the radical pathway, methanol decomposes via atomic hydrogen loss either to the methoxy radical (CH₃O) or to the hydroxymethyl radical (CH₂OH) [57,91]. Both radicals were found to react with nitrogen monoxide (NO) to form methyl nitrite (CH₃ONO; 2) and nitrosomethanol (H₂C(NO)OH; 4), respectively.

2.3. Non-equilibrium decomposition

Besides the isomerization (2.1.) and classical radical and molecular elimination channels (2.2.), the exposure of thin films of homogeneously mixed nitromethane (CH₃NO₂; 1) and of D₃-nitromethane (CD₃NO₂) to the ionizing radiation in form of energetic electrons and monochromatic photons (Lyman α; 10.2 eV) at 5 K revealed three more exotic high energy pathways [55], which have not been observed under collision-less conditions in the gas phase. These highly endoergic (by up to 440 kJ mol⁻¹) processes involve suprathreshold oxygen (O) (reaction (5)), hydrogen (H) (reaction (6)), and carbene (CH₂) (reaction (7)) formed in the decomposition of (CH₃NO₂; 1) and/or methyl nitrite (CH₃ONO; 2) (Fig. 5).



2.3.1. Atomic oxygen loss channel

Experiments on the decomposition of pure nitromethane (CH₃NO₂) and D₃-nitromethane (CD₃NO₂) ices at 5 K upon exposure to energetic electrons and Lyman α photons detected signal via PI-ReTOF-MS at *m/z* = 45 (CH₃NO; 45 amu; IE = 9.3 eV) and *m/z* = 48 (CD₃NO; 48 amu; IE = 9.3 eV) [80,81]. This signal could be attributed to nitrosomethane formed via atomic oxygen loss of nitromethane (CH₃NO₂; 61 amu) and D₃-nitromethane (CD₃NO₂; 64 amu), respectively. In homogeneously mixed nitromethane (CH₃NO₂) - D₃-nitromethane (CD₃NO₂) ices, *m/z* = 61 and *m/z* = 64, respectively, were also observed [55]. To form ground or excited state oxygen atoms, this channel is endoergic by 363 or 552 kJ mol⁻¹, respectively. Further evidence on the atomic oxygen loss channel was presented based on the identification of the ‘dimers’ of nitrosomethane and D₃-nitrosomethane at *m/z* = 90 and 96, respectively, in the form of (E)-azodioxy methane (IE = 8.6 eV). In irradiated nitromethane (CH₃NO₂) - D₃-nitromethane (CD₃NO₂) ices, (CH₃NO)₂ (*m/z* = 90), (CD₃NO)₂ (*m/z* = 96), and also (CH₃NOCD₃NO) (*m/z* = 93) was observed. Minor signal at *m/z* = 92 and 91 at levels of less than 10% compared to signal at *m/z* = 93 is likely the result of CH₃NO-CD₂HNO and CH₃NO-CH₂DNO dimerization. This in turn proposes the existence of CH₂DNO₂ and CD₂HNO₂ as discussed below. These dimerization reactions could take place in the condensed phase upon exposure to energetic electrons and photons. It is important to mention that in the TPD phase of the irradiated (D₃)-nitromethane ices, two peaks emerged at *m/z* = 45 and 48, respectively. Extensive PI-ReTOF-MS studies revealed the existence of two distinct isomers: nitrosomethane (CH₃NO; IE = 9.25 eV) and (trans) formaldehyde oxime (CH₂NOH; IE = 10.03 eV), which is less stable by about 50 kJ mol⁻¹ compared to nitrosomethane and likely formed by a keto-enol-type tautomerization *via* hydrogen shift from the carbon atom to the oxygen atom of the nitroso group of nitrosomethane. This pathway is similar to the keto-enol tautomerization of acetaldehyde (CH₃CHO) to vinyl alcohol (C₂H₃OH) in low temperature ices [92].

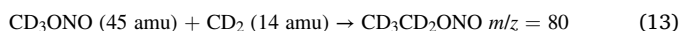
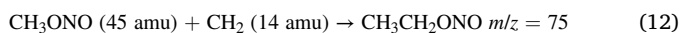
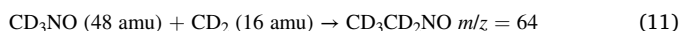
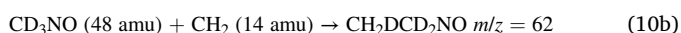
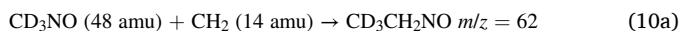
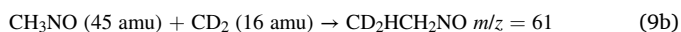
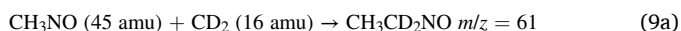
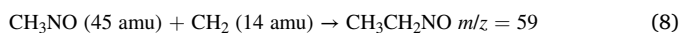
2.3.2. Atomic hydrogen loss channel

The PI-ReTOF-MS studies could verify the existence of free hydrogen atoms (reaction (6)). These free hydrogen atoms could be formed via highly endoergic carbon-hydrogen bond rupture in nitromethane (CH₃NO₂) and/or methyl nitrite (CH₃ONO). Note that ESR studies also provided compelling evidence of free hydrogen atoms (H) and of the nitromethyl (CH₂NO₂) radical demonstrating the existence of a high energy decomposition pathway, which is closed under collision-less conditions in the gas phase [90]. These findings could be replicated in D₃-nitromethane ices through the ESR detection of the D₂-nitromethyl

(CD₂NO₂) radical. Note that the methylene nitrite (CH₂ONO) radical was not reported in these ESR studies proposing that the methylene nitrite radical is not formed or concentrations are below the detection limit of our system. Consequently, the decomposition of nitromethane (CH₃NO₂) is expected to represent the dominant source of suprathreshold hydrogen atoms (reaction (6a)). In nitromethane (CH₃NO₂) - D3-nitromethane (CD₃NO₂) ices, recombination of deuterium atoms with the nitromethyl (CH₂NO₂) radical and of atomic hydrogen with the D2-nitromethyl (CD₂NO₂) radical should result in D1-nitromethane (CH₂DNO₂) and D2-nitromethane (CD₂HNO₂), respectively, as observed experimentally.

2.3.3. Carbene loss channel

The studies of the nitromethane (CH₃NO₂) and D3-nitromethane (CD₃NO₂) ices provided compelling evidence of molecular mass growth processes involving carbene (CH₂) and D2-carbene (CD₂) reactants likely formed via reaction (7). Carbene in its first excited singlet state (¹A₁) can insert barrierlessly into carbon-hydrogen bonds [93]. These mass growth processes by 14 amu and 16 amu are connected to the detection of *m/z* = 45 (CH₃NO; 45 amu; IE = 9.3 eV) versus 59 (CH₃CH₂NO; 59 amu; IE = 10.1 eV) and 61 (CH₃ONO; 61 amu; IE = 10.44 eV) versus 75 (CH₃CH₂ONO; 75 amu; IE = 10.53 eV) from the exposed nitromethane samples, which is also correlated with the mass-to-charge ratios of 48 (CD₃NO; 48 amu; IE = 9.3 eV) versus 64 (CD₃CD₂NO; 64 amu; IE = 10.1 eV) and 64 (CD₃ONO; 64 amu; IE = 10.44 eV) versus 80 (CD₃CD₂ONO; 80 amu; IE = 10.53 eV) in the D3-nitromethane ices reaching peak sublimation rates at about 160 K. These findings could also be verified in mixed nitromethane (CH₃NO₂) - D3-nitromethane (CD₃NO₂) ices through the identification of the carbene and D2-carbene insertion products into carbon-hydrogen/carbon-deuterium and carbon/nitrogen single bonds and detection of *m/z* = 59, 61, 62, and 64 (reactions (8)–(11)).



In support of the carbene insertion pathway, the authors also verified the molecular mass growth processes from methyl nitrite (CH₃ONO) to ethylnitrite (C₂H₅ONO) and n/iso-propylnitrite (C₃H₇ONO) along with the isotopically labeled counterparts. Note that since the ionization energies of the corresponding nitro isomers (e.g. IE (CH₃NO₂) = 11.08 eV, IE(C₂H₅NO₂) = 10.9 eV) is below the highest photon energy of 10.49 eV exploited for the photoionization, mass growth processes leading to nitro alkane isomers could not be explicitly elucidated. With respect to the alkyl nitrites, carbene (CH₂) and D2-carbene (CD₂) reaction with methyl nitrite (CH₃ONO; 61 amu) and D3-methyl nitrite (CD₃ONO; 64 amu), respectively, lead to signal at *m/z* = 75 (C₂H₅ONO⁺) and *m/z* = 80 (C₂D₅ONO⁺) [reactions (12) and (13)]. Likewise, insertion of carbene (CH₂) and D2-carbene (CD₂) into the carbon-hydrogen and/or carbon-nitrogen single bonds of D3-methyl nitrite (CD₃ONO; 64 amu) and methyl nitrite (CH₃ONO; 61 amu) resulted in signal at *m/z* = 78 (CD₃CH₂ONO⁺/CH₂DCD₂ONO⁺) and *m/z* = 77 (CH₃CD₂ONO⁺/CD₂HCH₂ONO⁺). It should be noted that smaller signal peaking at 160 K could also be found at *m/z* = 76 and 79; this signal could arise from H versus D and D versus H exchange pathways in the methylnitrite/D3-methylnitrite molecules followed by carbene and

D2-carbene insertion. Note that the D versus H and/or H versus D exchange can also take place in the nitromethane and D3-nitromethane prior to their isomerization to the (D3)-methylnitrite isomers. Nevertheless, these minor pathways clearly indicate the effectiveness of a carbon-hydrogen bond rupture in either the reactants ((D3)-nitromethane) or the nitrite isomers ((D3)-methyl nitrite) as suggested in reaction (7). Carbene insertion also lead to the detection of n/i-propyl nitrite (C₃H₇ONO) at *m/z* = 89.

Overall, three key non-equilibrium pathways (reactions (5) – (7)) were unraveled which are absent under collision-less conditions in the gas phase. The detection of three azodioxymethanes (CH₃NO)₂, (CD₃NO)₂, and CH₃NOCD₃NO verifies the presence of the corresponding nitrosomethane isomers (CH₃NO), which in turn are formed via atomic oxygen loss from their nitromethane precursor molecules via reaction (5) in strongly endoergic reactions [Δ_RG = +363/552 kJ mol⁻¹]. Further, carbene insertion lead to molecular mass growth processes as validated by the conversion of (D3)-nitrosomethane (CH₃NO/CD₃NO) to (D5)-nitrosoethane (CH₃CH₂NO/CD₃CD₂NO); isotopically mixed counterparts CH₃CD₂NO/CD₂HCH₂NO as well as CD₃CH₂NO/CH₂DCD₂NO suggest the reactions of D2-carbene and carbene with nitrosomethane and D3-nitrosomethane, respectively. Additional evidence is provided through the identification of the nitrosomethane (CH₃NO₂)/methylnitrite (CH₃ONO) reaction with carbene leading to nitroethane (C₂H₅NO₂)/ethylnitrite (C₂H₅ONO) together with their (partially) deuterated counterparts. Recall that these studies have not unraveled yet if carbene reacts with nitromethane to nitroethane followed by isomerization to ethylnitrite or if nitromethane isomerizes first to methylnitrite followed by reaction with carbene to ethylnitrite. Nevertheless, systematic mass growth processes via carbene insertion are evident.

2.4. Molecular mass growth process

With the help of deuterated nitromethane reactants, PI-ReTOF-MS exposed three classes of higher molecular weight products, which are uniquely formed in the condensed phase: (i) nitroso alkanes, (ii) alkyl nitrites, and (iii) higher molecular weight molecules (Fig. 5). As discussed in the previous section, a key molecular mass growth process to nitroso and nitrite compounds could be attributed to insertion of carbene (CH₂) into at least carbon-hydrogen bonds forming from nitrosomethane (CH₃NO) nitrosoalkanes: nitrosoethane (C₂H₅NO) and n/iso-nitrosopropane (C₃H₇NO). Starting with methylnitrite (CH₃ONO), carbene insertion lead to nitroalkanes: ethylnitrite (C₂H₅ONO) and n/iso-propylnitrite (C₃H₇ONO); these pathways are not feasible under collision less conditions in the gas phase. Even higher molecular weight products from 90 to 106 amu can be linked to the involvement of formally two nitromethane molecules. Upon exposure to energetic electrons and/or photons, nitromethane (CH₃NO₂; 61 amu) and nitrosomethane (CH₃NO; 45 amu) can emit a hydrogen atom yielding the nitromethyl (CH₂NO₂; 60 amu) and nitrosomethyl (CH₂NO; 44 amu) radicals. These processes are endoergic by 461 kJ mol⁻¹ and 464 kJ mol⁻¹. These radicals react forming a species of the chemical formula C₂H₄N₂O₃. Based on a radical – radical recombination, this molecule could be 1-nitroso-2-nitroethane (ONCH₂CH₂NO₂; 104 amu). Also, we detected ion counts at *m/z* = 91 potentially from the reaction of nitromethyl (CH₂NO₂; 60 amu) or its isomer with the methoxy radical (CH₃O; 31 amu) to methoxynitromethanol (CH₃O-CH₂NO₂; 91 amu). Further, the experiments detected signal at *m/z* = 90 and 106. This might be linked to ‘dimers’ of nitrosomethane, i.e. (CH₃NO-CH₃NO; 90 amu; IE = 8.6 eV), and of reaction products of nitrosomethane (CH₃NO; 45 amu) with nitromethane (CH₃NO₂; 61 amu) forming CH₃NO-CH₃NO₂ (106 amu). Nitrosomethane (CH₃NO) dimerizes easily forming (E)-azodioxymethane [94]. Signal at *m/z* = 106 is formally derived from reaction of a nitrosomethane (CH₃NO; 45 amu) with nitromethane (CH₃NO₂; 61 amu) yielding CH₃NO-CH₃NO₂ (106 amu). The nature of these isomers is still under investigation. Finally, in electron-irradiated

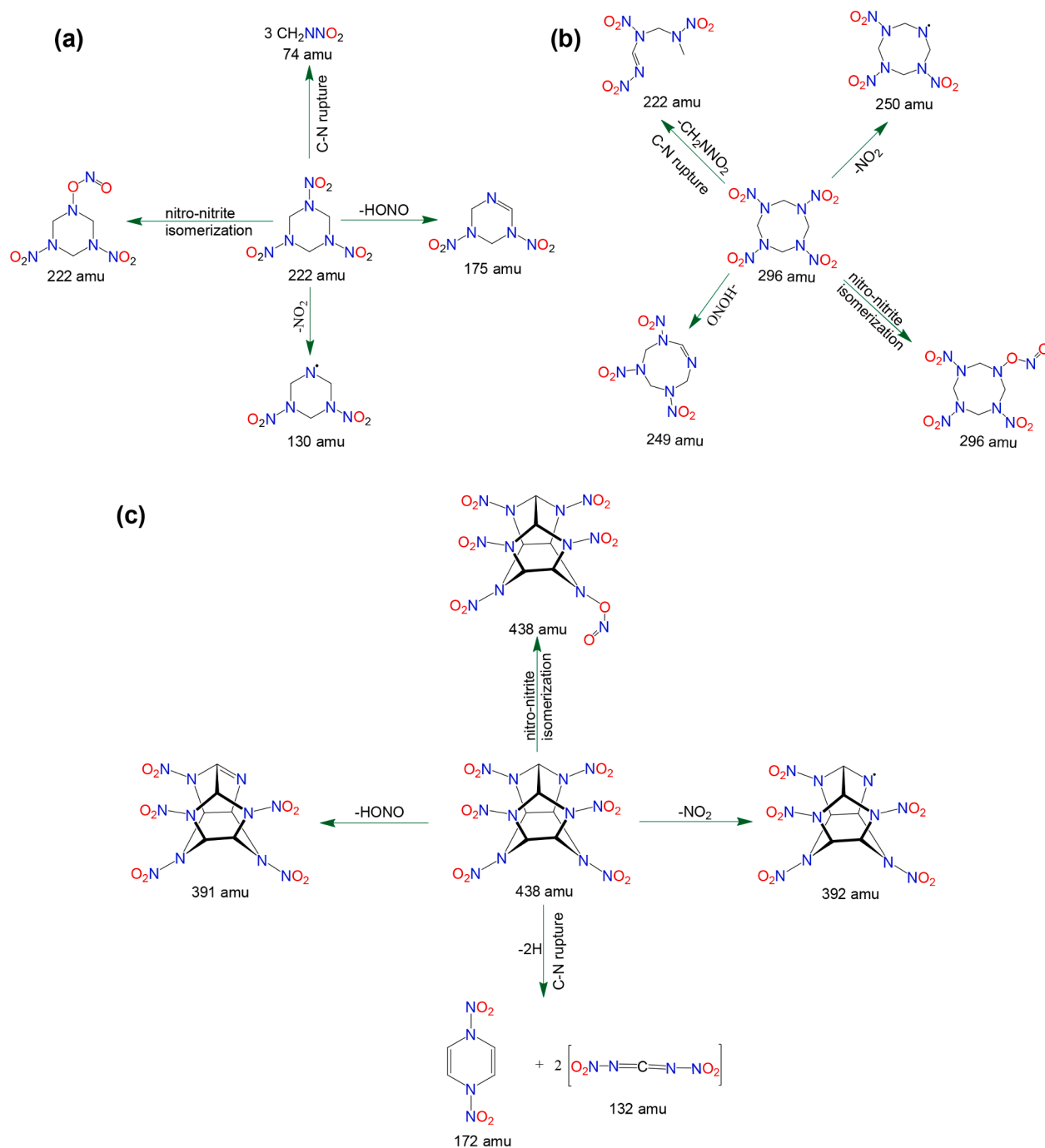


Fig. 6. Primary decomposition pathways of (a) 1,3,5-trinitro-1,3,5-triazinane (RDX), (b) 1,3,5,7-tetranitro-1,3,5,7-tetrazoctane (HMX) and (c) hexanitrohexaazaisowurtzitane (CL-20).

nitromethane ices, signal at $m/z = 135$ represents the highest ion observable. This can be formally assigned to a ‘trimer’ of nitroso-methane (CH₃NO; 45 amu) of hitherto unknown structure [80].

3. Future challenges and directions

Reflectron time-of-flight mass spectrometry coupled with tunable vacuum ultraviolet (VUV) single photon ionization (PI) of the subliming molecules (PI-ReTOF-MS) during the temperature programmed desorption (TPD) phase has been communicated as a versatile approach to untangle the isomerization, (non) equilibrium decomposition pathways, and molecular mass growth processes involved in the chemistry of solid nitromethane (CH₃NO₂). **First**, supported by infrared spectroscopy,

the temporal profiles and the kinetic fits suggest (pseudo) first order kinetics of the nitromethane (CH₃NO₂; 1) to methylnitrite (CH₃ONO; 2) isomerization. This isomerization is followed by two competing pathways: the molecular decomposition channel to formaldehyde (H₂CO) plus nitrosyl hydride (HNO) and the radical pathway to the methoxy radical (CH₃O) plus nitrogen monoxide (NO). These mechanisms are consistent with previous gas phase studies and computational investigations: the energized nitromethane initially enters the dissociation channel CH₃...NO₂ with the calculated C-N bond length at about 4.58 Å [3]. The fragments re-orient and recombine to form the *cis*-CH₃ONO isomer via roaming, which can then result in the molecular and radical fragmentation pathways as discussed above. In the ice matrix, the cage effect of two initially formed radical recombining is reflected in reaction

mechanisms, which do not exist in gas phase reactions under single collision conditions, where the nascent products ‘fly apart’ or undergo prior reactions via ‘roaming’. **Second**, three exotic isomers of nitromethane (CH_3NO_2 ; **1**) and methyl nitrite (CH_3ONO ; **2**) were detected: aci-nitromethane ($\text{H}_2\text{C}=\text{N}(\text{O})\text{OH}$; **3**), nitrosomethanol ($\text{H}_2\text{C}(\text{NO})\text{OH}$; **4**), N-hydroxyoxaziridine ($\text{c-CH}_2\text{NOH}(\text{O})$; **5**) suggesting the presence of hydrogen and hydroxyl shifts, which have not been exposed in previous gas phase studies exploiting molecular beams. **Third**, besides these isomerization and classical radical and molecular elimination channels, the experiments in the condensed phase revealed three high energy pathways [55,90], which have not been observed under collision-less conditions in the gas phase. These highly endoergic (by up to 440 kJ mol⁻¹) processes involve the generation of suprathreshold oxygen (O), hydrogen (H), and carbene (CH_2) formed in the decomposition of (CH_3NO_2 ; **1**) and/or methyl nitrite (CH_3ONO ; **2**). **Finally**, key molecular mass growth processes were attributed to insertion of carbene (CH_2) into carbon-hydrogen bonds forming from nitrosomethane (CH_3NO) a homologues series of **nitrosoalkanes**: nitrosoethane ($\text{C}_2\text{H}_5\text{NO}$) and nitrosopropane ($\text{C}_3\text{H}_7\text{NO}$). Also, starting with methyl nitrite (CH_3ONO), carbene insertion can lead to a homologues series of **nitritoalkanes**: ethyl nitrite ($\text{C}_2\text{H}_5\text{ONO}$) and propyl nitrite ($\text{C}_3\text{H}_7\text{ONO}$). Finally, these studies identified molecules, which necessitate the reaction of (fragments of) two and three nitromethane building blocks, which do not exist in gas phase reactions. Overall, these condensed phase studies vastly undersized the detailed understanding to a very multifaceted issue that has only been skimmed over in the gas phase by exposing key reaction mechanisms in the condensed phase, which are not feasible in the gas phase due to the ‘single collision conditions’ exploited. Further analysis on the decomposition of nitromethane in the condensed phase is critical in order to understand the full complexity of the process. These experiments will rely on the coherent use of molecular selective ionization utilizing tunable vacuum ultraviolet light and *ab initio* calculations as the decomposition of nitromethane in the solid state obviously results in molecules whose ionization energies have yet to be examined experimentally. Further, it is desirable to combine these experimental studies with molecular dynamics calculations. Recent dynamics studies by Perriot et al. [95] also proposed the existence of unconventional reaction intermediates such as of aci-nitromethane ($\text{H}_2\text{C}=\text{N}(\text{O})\text{OH}$; **3**) and formal ‘dimers’ of nitrosomethane (CH_3NO), but these studies failed to link the computational results to recent experimental data [79,82].

Once the experimental results of the ‘simple’ nitromethane system have been successfully benchmarked with dynamics simulations, these studies can be expanded to ‘real’ energetic materials and explosives such as 1,3,5-trinitro-1,3,5-triazinane (RDX) [96–98], 1,3,5,7-tetranitro-1,3,5,7-tetrazoctane (HMX) [99,100], and hexanitrohexaazaisowurtzitane (CL-20) [101–104]. Decomposition of these explosives are more complex owing to the several competing reaction channels and high number of radicals and product species formed during the decomposition. For instance, unimolecular decomposition of RDX, HMX and CL-20 can initiate through four primary steps (1) N-NO₂ bond cleavage resulting in the formation of nitrogen dioxide (NO₂) along with a N-centered radical, (2) molecular elimination channel yielding nitrous acid (HONO) and unsaturated ring species, (3) nitro-nitrite rearrangement followed by NO loss and (4) ring opening pathway leading to methylene nitramine ($\text{H}_2\text{C}(\text{NO})\text{NO}_2$) (Fig. 6a-c) [99,100,103–109]. These reaction steps are often accompanied by several secondary reactions leading to large number of products for example, dissociation of RDX generate products having molecular weight ranging from 18 to 191 amu [96,97,105,107,110–112]. Recent studies exploiting PI-ReTOF-MS revealed the necessity to exploit isomer selective photoionization schemes of the reaction products as the only means to discount previous problematic assignment of, e.g. diazomethane (CH_2NN ; 42 amu) as the decomposition product of RDX as determined with electron impact mass spectrometry [111,113,114], whereas PI-ReTOF-MS provided compelling evidence that $m/z = 42$ is linked to ketene (H_2CCO), but not to diazomethane (CH_2NN) [98]. Future experimental advances should link

PI-ReTOF-MS to synchrotron facilities to take advantage of beamlines operating with tunable VUV light [115,116]. Further, although pump–probe experiments are widely used in the gas phase to explore, for instance, the photodissociation dynamics of organics such as cytosine and 1,2-cyclohexanedione [117–119] however, they have not been exploited extensively in low-temperature targets to elucidate in particular the decomposition of energetic materials. Investigation of photodissociation of explosives such as RDX employing ultrafast pump–probe laser spectroscopy can provide information on time-dependent decomposition dynamics.

CRedit authorship contribution statement

Santosh K. Singh: Investigation, Data curation, Formal analysis, Visualization, Writing - review & editing. **Ralf I. Kaiser**: Conceptualization, Writing - original draft, Writing - review & editing, Funding acquisition, Supervision.

Declaration of Competing Interest

The authors declare that they have no known competing financial interests or personal relationships that could have appeared to influence the work reported in this paper.

Acknowledgements

The work was supported by the US Army Research Office (W911NF1810438). The W. M. Keck Foundation and the University of Hawaii at Manoa financed the construction of the experimental setup. RIK acknowledges the coauthors and collaborators that contributed to the published work mentioned here.

References

- [1] G.F. Adams, R.W. Shaw, *Annu. Rev. Phys. Chem.* 43 (1992) 311.
- [2] D.S. George Olah (Ed.), *Chemistry of Energetic Materials*, Academic Press, San Diego, 1991.
- [3] Z. Homayoon, J.M. Bowman, *J. Phys. Chem. A* 117 (2013) 11665.
- [4] M.L. McKee, *J. Am. Chem. Soc.* 108 (1986) 5784.
- [5] F. Guo, X.-L. Cheng, H. Zhang, *J. Phys. Chem. A* 116 (2012) 3514.
- [6] A.K. Sikder, N. Sikder, *J. Hazard. Mater.* 112 (2004) 1.
- [7] D.M. Badgular, M.B. Talawar, S.N. Asthana, P.P. Mahulikar, *J. Hazard. Mater.* 151 (2008) 289.
- [8] Y.-X. Zhang, S.H. Bauer, *J. Phys. Chem. B* 101 (1997) 8717.
- [9] J.M. Winey, Y.M. Gupta, *J. Phys. Chem. B* 101 (1997) 10733.
- [10] J.M. Winey, Y.M. Gupta, *J. Phys. Chem. A* 101 (1997) 9333.
- [11] V. Bouyer, I. Darbord, P. Hervé, G. Baudin, C. Le Gallic, F. Clément, G. Chavent, *Combust. Flame* 144 (2006) 139.
- [12] S. Kelzenberg, N. Eisenreich, W. Eckl, V. Weiser, *Propellants Explos. Pyrotec.* 24 (1999) 189.
- [13] E. Boyer, K.K. Kuo, *Proc. Combust. Inst.* 31 (2007) 2045.
- [14] Q. Zhang, W. Li, D.-C. Lin, N. He, Y. Duan, *J. Hazard. Mater.* 185 (2011) 756.
- [15] R.P. Singh, R.D. Verma, D.T. Meshri, J.n.M. Shreeve, *Angew. Chem. Int. Ed.* 45 (2006) 3584.
- [16] G.D. Kozak, *Propellants Explos. Pyrotec.* 30 (2005) 291.
- [17] L.E. Fried, M.R. Manaa, J.P. Lewis, *Overviews of Recent Research on Energetic Materials*, p. 275.
- [18] J.C. Oxley, *Energetic Materials Part 1. Decomposition, Crystal and Molecular Properties, Theoretical and Computational Chemistry*, 2003.
- [19] B.B. Vogelsanger, Presented at the 36th International Annual Conference of ICT, Karlsruhe, Germany, 2005.
- [20] E.W. Deschambault, D., F. Peugeot, P. Touze, Presented at the 37th International Annual Conference of ICT, Karlsruhe, Germany, 2006.
- [21] W.d.B. Klerk, G.R., H. Keizers, Presented at the 37th International Annual Conference of ICT, Karlsruhe, Germany, 2006.
- [22] A. Bhattacharya, Y. Guo, E.R. Bernstein, *Acc. Chem. Res.* 43 (2010) 1476.
- [23] T.B. Brill, K.J. James, *Chem. Rev.* 93 (1993) 2667.
- [24] R.W. Beal, T.B. Brill, *Appl. Spectrosc.* 59 (2005) 1194.
- [25] R.W.A.B. Shaw, B.A. Thomas, Donald L. Thompson, *Overviews of Recent Research on Energetic Materials*. World Scientific, (2005).
- [26] R.I. Kaiser, *Chem. Rev.* 102 (2002) 1309.
- [27] Y.-z. Sun, Y. Shu, T. Xu, M. Shui, Z. Zhao, Y.d. Gu, X. Wang, *Cent. Eur. J. Energ. Mater.* 9 (2012) 411.
- [28] D. Furman, R. Kosloff, F. Dubnikova, S.V. Zybin, W.A. Goddard, N. Rom, B. Hirshberg, Y. Zeiri, *J. Am. Chem. Soc.* 136 (2014) 4192.
- [29] A.B. Bass, H., *Formation and Trapping of Free Radicals*, Acad Press, NY, 1960.

- [30] A.S.B. Shterberg, A. A., Presented at the 35th International Pyrotechnics Seminar, Fort Collins, Colorado, July 13- 18, (2008).
- [31] A.M. Wodtke, E.J. Hints, Y.T. Lee, *J. Chem. Phys.* 84 (1986) 1044.
- [32] L.J. Butler, D. Krajnovich, Y.T. Lee, G.S. Ondrey, R. Bersohn, *J. Chem. Phys.* 79 (1983) 1708.
- [33] K.Q. Lao, E. Jensen, P.W. Kash, L.J. Butler, *J. Chem. Phys.* 93 (1990) 3958.
- [34] Y.Q. Guo, A. Bhattacharya, E.R. Bernstein, *J. Phys. Chem. A* 113 (2009) 85.
- [35] Y. Kohge, T. Hanada, M. Sumida, K. Yamasaki, H. Kohguchi, *Chem. Phys. Lett.* 556 (2013) 49.
- [36] A. Dey, R. Fernando, C. Abeyssekera, Z. Homayoon, J.M. Bowman, A.G. Suits, *J. Chem. Phys.* 140 (2014), 054305.
- [37] I.M. Napier, R.G.W. Norrish, *Proc. Roy. Soc. London. Ser. A. Math. Phys. Sci.* 299 (1967) 317.
- [38] E. Hirschlaff, R.G.W. Norrish, *J. Chem. Soc. (Resumed)* (1936) 1580.
- [39] B.H. Rockney, E.R. Grant, *J. Chem. Phys.* 79 (1983) 708.
- [40] A.M. Renlund, W.M. Trott, *Chem. Phys. Lett.* 107 (1984) 555.
- [41] J.C. Mialocq, J.C. Stephenson, *Chem. Phys.* 106 (1986) 281.
- [42] D.B. Moss, K.A. Trentelman, P.L. Houston, *J. Chem. Phys.* 96 (1992) 237.
- [43] J.B. Simeonsson, G.W. Lemire, R.C. Sausa, *Anal. Chem.* 66 (1994) 2272.
- [44] G.D. Greenblatt, H. Zuckermann, Y. Haas, *Chem. Phys. Lett.* 134 (1987) 593.
- [45] E.A. Wade, K.E. Reak, S.L. Li, S.M. Clegg, P. Zou, D.L. Osborn, *J. Phys. Chem. A* 110 (2006) 4405.
- [46] R.S. Zhu, M.C. Lin, *Chem. Phys. Lett.* 478 (2009) 11.
- [47] R.S. Zhu, P. Raghunath, M.C. Lin, *J. Phys. Chem. A* 117 (2013) 7308.
- [48] T. Nagata, M. Suzuki, K. Suzuki, T. Kondow, K. Kuchitsu, *Chem. Phys.* 88 (1984) 163.
- [49] R.E. Rebert, N. Slagg, *Bulletin des Sociétés Chimiques Belges* 71 (1962) 709.
- [50] B.H.J. Bielski, R.B. Timmons, *J. Phys. Chem.* 68 (1964) 347.
- [51] H.W. Brown, G.C. Pimentel, *J. Chem. Phys.* 29 (1958) 883.
- [52] M.E. Jacox, *J. Phys. Chem.* 88 (1984) 3373.
- [53] S.-P. Han, A.C.T. van Duin, W.A. Goddard, A. Strachan, *J. Phys. Chem. B* 115 (2011) 6534.
- [54] M. Citroni, F. Datchi, R. Bini, M. Di Vaira, P. Pruzan, B. Canny, V. Schettino, *J. Phys. Chem. B* 112 (2008) 1095.
- [55] R.I. Kaiser, P. Maksyutenko, *Chem. Phys. Lett.* 631–632 (2015) 59.
- [56] S. Maity, R.I. Kaiser, B.M. Jones, *Phys. Chem. Chem. Phys.* 17 (2015) 3081.
- [57] S. Maity, R.I. Kaiser, B.M. Jones, *Faraday Discuss.* 168 (2014) 485.
- [58] A.M. Turner, M.J. Abplanalp, S.Y. Chen, Y.T. Chen, A.H.H. Chang, R.I. Kaiser, *Phys. Chem. Chem. Phys.* 17 (2015) 27281.
- [59] M.J. Abplanalp, M. Förstel, R.I. Kaiser, *Chem. Phys. Lett.* 644 (2016) 79.
- [60] C.J. Bennett, S.J. Broton, B.M. Jones, A.K. Misra, S.K. Sharma, R.I. Kaiser, *Anal. Chem.* 85 (2013) 5659.
- [61] A. Bergantini, M.J. Abplanalp, P. Pokhilko, A.I. Krylov, C.N. Shingledecker, E. Herbst, R.I. Kaiser, *Astrophys. J.* 860 (2018) 108.
- [62] B.M. Jones, R.I. Kaiser, *J. Phys. Chem. Lett.* 4 (2013) 1965.
- [63] M.J. Abplanalp, R.I. Kaiser, *Phys. Chem. Chem. Phys.* 21 (2019) 16949.
- [64] A. Bergantini, S. Góbi, M.J. Abplanalp, R.I. Kaiser, *Astrophys. J.* 852 (2018) 70.
- [65] C. Zhu, R. Frigge, A.M. Turner, M.J. Abplanalp, B.-J. Sun, Y.-L. Chen, A.H. Chang, R.I. Kaiser, *Phys. Chem. Chem. Phys.* 21 (2019) 1952.
- [66] R. Hilbig, R. Wallenstein, *IEEE J. Quant. Electron.* 17 (1981) 1566.
- [67] R. Hilbig, G. Hilber, A. Lago, B. Wolff, R. Wallenstein, *Tunable Coherent VUV Radiation Generated by Nonlinear Optical Frequency Conversion in Gases*, SPIE, 1986.
- [68] H. Egsgaard, L. Carlsen, H. Florêncio, T. Drewello, H. Schwarz, *Berichte der Bunsengesellschaft für physikalische Chemie* 93 (1989) 76.
- [69] J.N. Murrell, B. Vidal, M.F. Guest, *J. Chem. Soc. Faraday Trans. 2* (71) (1975) 1577.
- [70] S. Sengupta, Y. Indulkar, A. Kumar, S. Dhanya, P.D. Naik, P.N. Bajaj, *J. Phys. Chem. A* 112 (2008) 12572.
- [71] C.-Y. Sung, L.J. Broadbelt, R.Q. Snurr, *J. Phys. Chem. C* 113 (2009) 15643.
- [72] L. Wang, C. Yi, H. Zou, J. Xu, W. Xu, *Chem. Phys.* 367 (2010) 120.
- [73] R.P. Mueller, J.R. Huber, *J. Phys. Chem.* 87 (1983) 2460.
- [74] Y. Jianguo, L. Ruozhuang, *Acta Phys. -Chim. Sin.* 5 (1989) 340.
- [75] G.H. Kalkanis, G.C. Shields, *J. Phys. Chem.* 95 (1991) 5085.
- [76] D.N. Shin, D.J. Koh, K.T. Kim, I.P. Hamilton, *Catal. Today* 119 (2007) 209.
- [77] W.-F. Hu, T.-J. He, D.-M. Chen, F.-C. Liu, *J. Phys. Chem. A* 106 (2002) 7294.
- [78] J.-X. Zhang, J.-Y. Liu, Z.-S. Li, C.-C. Sun, *J. Comput. Chem.* 26 (2005) 807.
- [79] P. Maksyutenko, M. Förstel, P. Crandall, B.-J. Sun, M.-H. Wu, A.H.H. Chang, R. I. Kaiser, *Chem. Phys. Lett.* 658 (2016) 20.
- [80] R.I. Kaiser, P. Maksyutenko, *J. Phys. Chem. C* 119 (2015) 14653.
- [81] P. Maksyutenko, L.G. Muzangwa, B.M. Jones, R.I. Kaiser, *Phys. Chem. Chem. Phys.* 17 (2015) 7514.
- [82] S.K. Singh, T.-Y. Tsai, B.-J. Sun, A.H.H. Chang, A.M. Mebel, R.I. Kaiser, *J. Phys. Chem. Lett.* 11 (2020) 5383.
- [83] K.S. Williamson, D.J. Michaelis, T.P. Yoon, *Chem. Rev.* 114 (2014) 8016.
- [84] J. Aubé, *Chem. Soc. Rev.* 26 (1997) 269.
- [85] M. Poláček, M. Sadilek, F. Tureček, *Int. J. Mass Spectrom.* 195-196 (2000) 101.
- [86] J. Sauer, *Tetrahedron* 35 (1979) 2109.
- [87] A. Rauk, *J. Am. Chem. Soc.* 103 (1981) 1023.
- [88] W.D. Emmons, *J. Am. Chem. Soc.* 79 (1957) 5739.
- [89] F.A. Davis, A.C. Sheppard, *Tetrahedron* 45 (1989) 5703.
- [90] Y.A. Tsegaw, W. Sander, R.I. Kaiser, *J. Phys. Chem. A* 120 (2016) 1577.
- [91] S. Góbi, P.B. Crandall, P. Maksyutenko, M. Förstel, R.I. Kaiser, *J. Phys. Chem. A* 122 (2018) 2329.
- [92] M.J. Abplanalp, S. Gozem, A.I. Krylov, C.N. Shingledecker, E. Herbst, R.I. Kaiser, *Proc. Natl. Acad. Sci. USA* 113 (2016) 7727.
- [93] R.D. Bach, M.D. Su, E. Aldabbagh, J.L. Andres, H.B. Schlegel, *J. Am. Chem. Soc.* 115 (1993) 10237.
- [94] F.A. Thomassy, F.W. Lampe, *J. Phys. Chem.* 74 (1970) 1188.
- [95] R. Perriot, M.J. Cawkwell, E. Martinez, S.D. McGrane, *J. Phys. Chem. A* 124 (2020) 3314.
- [96] S.K. Singh, C. Zhu, V. Vuppuluri, S.F. Son, R.I. Kaiser, *J. Phys. Chem. A* 123 (2019) 9479.
- [97] S.K. Singh, V. Vuppuluri, S.F. Son, R.I. Kaiser, *J. Phys. Chem. A* (2020).
- [98] S.K. Singh, J. La Jeunesse, V. Vuppuluri, S.F. Son, B.-J. Sun, Y.-L. Chen, A.H. Chang, A.M. Mebel, R.I. Kaiser, *ChemPhysChem* 21 (2020) 837.
- [99] M. Greenfield, Y.Q. Guo, E.R. Bernstein, *Chem. Phys. Lett.* 430 (2006) 277.
- [100] C.-C. Ye, Q. An, W.-Q. Zhang, W.A. Goddard, *J. Phys. Chem. C* 123 (2019) 9231.
- [101] N.H. Naik, G.M. Gore, B.R. Gandhe, A.K. Sikder, *J. Hazard. Mater.* 159 (2008) 630.
- [102] M. Geetha, U.R. Nair, D.B. Sarwade, G.M. Gore, S.N. Asthana, H. Singh, *J. Therm. Anal. Calorim.* 73 (2003) 913.
- [103] O. Isayev, L. Gorb, M. Qasim, J. Leszczynski, *J. Phys. Chem. B* 112 (2008) 11005.
- [104] S.K. Kumar, P. Ashutosh, A.A. Vargeese, *J. Phys. Chem. A* 123 (2019) 4014.
- [105] D. Chakraborty, R.P. Muller, S. Dasgupta, W.A. Goddard, *J. Phys. Chem. A* 104 (2000) 2261.
- [106] D. Chakraborty, R.P. Muller, S. Dasgupta, W.A. Goddard, *J. Phys. Chem. A* 105 (2001) 1302.
- [107] I.V. Schweigert, *J. Phys. Chem. A* 119 (2015) 2747.
- [108] Y.Q. Guo, M. Greenfield, E.R. Bernstein, *J. Chem. Phys.* 122 (2005), 244310.
- [109] L. Lin-lin, S.-Q. Hu, *J. Energ. Mater.* 37 (2019) 154.
- [110] A. Bhattacharya, E.R. Bernstein, *J. Phys. Chem. A* 115 (2011) 4135.
- [111] X. Zhao, E.J. Hints, Y.T. Lee, *J. Chem. Phys.* 88 (1988) 801.
- [112] R.W. Molt, T. Watson, A.P. Bazanté, R.J. Bartlett, N.G.J. Richards, *Phys. Chem. Chem. Phys.* 18 (2016) 26069.
- [113] J.T. Dickinson, L.C. Jensen, D.L. Doering, R. Yee, *J. Appl. Phys.* 67 (1990) 3641.
- [114] T.B. Tang, M.M. Chaudhri, C.S. Rees, S.J. Mullock, *J. Mater. Sci.* 22 (1987) 1037.
- [115] L. Zhao, R.I. Kaiser, B. Xu, U. Ablikim, M. Ahmed, M.M. Evseev, E.K. Bashkurov, V. N. Azayov, A.M. Mebel, *Angew. Chem. Int. Ed.* 59 (2020) 4051.
- [116] L. Zhao, T. Yang, R.I. Kaiser, T.P. Troy, M. Ahmed, D. Belisario-Lara, J.M. Ribeiro, A.M. Mebel, *J. Phys. Chem. A* 121 (2017) 1261.
- [117] M. Kawade, A. Saha, H.P. Upadhyaya, A. Kumar, P.D. Naik, *J. Phys. Chem. A* 117 (2013) 2415.
- [118] C. Hu, L. Wang, Y. Wang, Y. Tang, J. Long, B. Zhang, *Chem. Phys. Lett.* 658 (2016) 134.
- [119] M. Broquier, S. Soorkia, G. Pino, C. Dedonder-Lardeux, C. Jouvet, G. Grégoire, *J. Phys. Chem. A* 121 (2017) 6429.



Santosh K. Singh received his Ph.D. in Chemistry from the Indian Institute of Science Education and Research, Pune (India) in 2018. He worked with Professor Alok Das during his Ph.D. on exploring weak $n \rightarrow \pi^*$ non-covalent interaction employing gas-phase laser spectroscopy and quantum chemical calculations. After finishing Ph.D., he joined the Department of Chemistry at the University of Hawaii at Manoa (USA) to pursue his postdoctoral research under the supervision of Professor Ralf I. Kaiser. His current research interests include understanding the decomposition mechanisms and kinetics of energetic materials in the condensed phase employing a surface science machine and photoionization.



Ralf I. Kaiser received his Ph.D. in Chemistry from the University of Münster (Germany) in 1994 and conducted postdoctoral work at UC Berkeley (Department of Chemistry). During 1997–2000 he received a fellowship from the German Research Council (DFG) to perform his Habilitation at the Department of Physics (University of Chemnitz, Germany) and Institute of Atomic and Molecular Sciences (Academia Sinica, Taiwan). He joined the Department of Chemistry at the University of Hawai'i at Manoa in 2002, where he is currently Professor of Chemistry and Director of the W. M. Keck Research Laboratory in Astrochemistry. He was elected Fellow of the Royal Astronomical Society (UK), the Royal Society of Chemistry (UK), the American Physical Society (APS), the American Association for the Advancement of Science (AAAS), the Institute of Physics (UK), and of the American Chemical Society (ACS). His research interests include reaction dynamics and kinetics (gas phase, liquids, ices), astrochemistry, astrobiochemistry, combustion chemistry, and material sciences.